Facile synthesis of palladium and gold nanoparticles by using dialdehyde nanocellulose as template and reducing agent

Kaitao Zhang[a,b], Minggui Shen[b,c], He Liu[b,c], Shibin Shang[b, c], Dan Wang[b,c, *] and Henrikki Liimatainen[a]

a. Fiber and Particle Engineering Research Unit, University of Oulu, P.O. Box 4300, FI-90014, Finland

b. Institute of Chemical Industry of Forest Products, CAF; Key and Open Lab of Forest Chemical Engineering, SFA, Nanjing 210042, China

c. Research Institute of Forestry New Technology, CAF, Beijing 100091, China

Abstract

Cellulose nanofibrils (CNFs) were firstly prepared by 2,2,6,6-tetramethylpiperidine-1-oxyl (TEMPO) oxidation and further oxidized to 2,3-dialdehyde nanocelluloses (DANCs) by periodate oxidation. Furthermore, by using DANCs as reducing as well as stabilizing agent, palladium (Pd) and gold (Au) nanoparticles (NPs) supported on nanocellulose (PdNPs@NC and AuNPs@NC) were synthesized, respectively. The reduction of Pd or Au ions to its metallic form by DANCs was confirmed by UV-vis spectra, XRD, and XPS. TEM results showed that Pd and Au NPs were homogenously deposited onto cellulose nanofibrils, respectively. The catalytic performance of PdNPs@NC was further investigated by Suzuki coupling reaction. The product yield of the Suzuki coupling reaction between aryl

* Corresponding author (Dan Wang) at : Institute of Chemical Industry of Forestry Products, Chinese Academy of Forestry, NO.16 Suojin Wucun, Nanjing, China. Tel.: +86 025 85482452; fax.: +86 025 85482499. *E-mail address:* kaitao.zhang@oulu.fi (K. Zhang), shenminggui@sina.com (M. Shen), liuheicifp@caf.ac.cn (H. Liu), shangsb@hotmail.com (S. Shang), wgdan@163.com (D. Wang), henrikki.liimatainen@oulu.fi (H. Liimatainen).

bromides and phenyl boronic acid was more than 90% after 1 h with 0.1 mol% PdNPs@NC catalyst, which demonstrated that the synthesized PdNPs@NC nanohybrid could be successfully applied in Suzuki coupling reaction with an efficient catalytic activity.

Keywords: Palladium; Gold; Nanoparticles; Cellulose nanofibrils; Catalysis; Aldehyde

1. Introduction

Noble metal nanoparticles, being totally distinct from their bulk metal equivalents, have attracted considerable attention because of their unique properties such as optical(Wang, Ye, Iocozzia, Lin, & Lin, 2016; Yu et al., 2017), magnetic, and electronic activities (Loh, 2016) and their high catalytic performances in many chemical reactions (Dong et al., 2015; Long, Thi, Yong, Nogami, & Ohtaki, 2013; Sarina, Waclawik, & Zhu, 2013). The synthesis of noble metal nanoparticles has been an important research topic in the field of nanoscience over the past decades (Wu, Kuang, Zhang, & Chen, 2011). Palladium nanoparticles (Pd NPs) are well known for their excellent catalytic activity in C-C cross-coupling reactions including Suzuki, Heck, Sonogashira and Stille reactions (Phan, Van Der Sluys, & Jones, 2006; Xu, Wu, & Zhu, 2008). To date, such reactions have been frequently employed in the synthesis of pharmaceuticals, agrochemicals, dyes and other products (Hassan, Sévignon, Gozzi, Schulz, & Lemaire, 2002). Among various cross-coupling reactions, Suzuki cross-coupling reactions of aryl halides with arylboronic acids have become the prevailing technique, as it is one of the most efficient methods for construction of biaryl compounds in organic synthesis (Kumbhar, Jadhav, Kamble, Rashinkar, &

Salunkhe, 2013). Likewise, gold nanoparticles (Au NPs) have attracted increasing interest due to their catalytic properties in various organic transformation reactions, including the CO oxidation, aerobic oxidation of alcohols, C−C coupling reactions and reduction reactions via transfer hydrogenation (Chen, Cao, Quinlan, Berry, & Tam, 2015; Chen et al., 2015). However, both Pd and Au nanoparticles suffer from agglomeration in solution due to their large specific surface areas (Wu et al., 2013). One strategy to stabilize metal nanoparticles is by employing capping agents such as thiols, carboxylate ligands, surfactants and polyelectrolytes (Chen et al., 2015). Most capping agents, however, are non-biodegradable polymers or potentially toxic chemicals (Shi et al., 2015). Another method to avoid agglomeration is by means of the immobilization of metal nanoparticles onto solid matrixes including carbon (Liu, Yang, Liu, Ye, & Wei, 2017), silica (Shimizu et al., 2004), metal oxide (Del Zotto & Zuccaccia, 2017), polymer, *etc.* (Yan et al., 2016). Polymeric supports are attractive due to a greater number of active sites such as carboxylate and amino in the structure (Chen et al., 2015). As the most abundant organic polymer in nature, cellulose has been extensively used as bio-templates for metal nanoparticles (He, Kunitake, & Nakao, 2003; Y. Li et al., 2017; H. Liu, Song, Shang, Song, & Wang, 2012; Van Rie & Thielemans, 2017).

Nanocellulose (NC), produced via chemical or physical approaches from vegetal or bacterial cellulose, mainly includes three different types, i.e., cellulose nanocrystals (CNCs), cellulose nanofibrils (CNFs) and bacterial cellulose (BC). (Li et al., 2015; Li, Sirviö, Haapala, & Liimatainen, 2017; Sirviö, Visanko, & Liimatainen, 2015; Sirvio

& Visanko, 2017; Suopajärvi, Sirviö, & Liimatainen, 2017; Visanko et al., 2017; Zhang et al., 2016). Nanocellulose has emerged as an attractive candidate for supporting metal NPs due to its high surface area, environmental sustainability and biodegradability (Hu, Meng, Liu, Fu, & Lucia, 2017; Kaushik & Moores, 2016; Wu et al., 2016; Xiong, Lu, Zhang, Zhou, & Zhang, 2013; Yan et al., 2016; Zhou et al., 2012). The most common preparation technique for the fabrication of noble metal NPs/nanocellulose hybrids is the treatment of noble metal salts with reducing agents in the presence of nanocellulose (Cirtiu, Dunlop-Briere, & Moores, 2011; Ghaderi, Gholinejad, & Firouzabadi, 2016; Koga et al., 2010; Liu et al., 2012; Van Rie & Thielemans, 2017). However, the reducing agents employed such as $NaBH_4$ and H_2 would be hazardous or dangerous (Wu et al., 2013; Wu et al., 2014). So far, several methods of reduction of metal nanoparticles by using nanocellulose as reducing agent have been reported (Benaissi, Johnson, Walsh, & Thielemans, 2010; Y. Y. Dong, Liu, Liu, Meng, & Ma, 2017; Fu, Deng, Ma, & Yang, 2016; Z. Hu, Q. Meng, R. Liu, S. Fu, & L. A. Lucia, 2017). Rezayat et al. (2014) prepared Pd NPs through nanocellulose-induced reduction of Pd precursors in subcritical and supercritical carbon dioxide ($scCO_2$). Likewise, Pd and Au NPs were synthesized in a hydrothermal system by using neat nanocellulose as both supporting matrix and reductant (Wu et al., 2013; Wu et al., 2014). Nonetheless, these methods still require harsh or complicated conditions (in $scCO_2$ or hydrothermal system).

Nanocellulose surface possesses many reactive hydroxyl groups, which can be utilized for further chemical modification. 2, 3-dialdehyde cellulose (DAC) can be

obtained by using periodate as oxidant to oxidize vicinal hydroxyl groups of cellulose at positions 2 and 3 to aldehyde groups (Liimatainen, Sirvio, Pajari, Hormi, & Niinimaki, 2013; Mou, Li, Wang, Cha, & Jiang, 2017; Sirvio, Liimatainen, Niinimaki, & Hormi, 2011). Wu, Kuga and Huang (2008) and Drogat et al. (2011) reported that Ag NPs could be produced and coated on nanocellulose while introducing DAC as reductant. As we know that the reduction potential of Pd (0.915 V) and Au (1.50 V) ion are higher than that of silver (0.8 V) (Nadagouda & Varma, 2008). Therefore, it would be possible to reduce Pd or Au ions to metallic forms by utilizing aldehyde groups on the surface of DAC. In the present study, cellulose nanofibrils (CNFs) were firstly prepared by 2,2,6,6-tetramethylpiperidine-1-oxyl (TEMPO) oxidation and further oxidized to 2,3-dialdehyde nanocellulose (DANCs) by sodium periodate. Pd NPs and Au NPs supported onto nanocellulose (PdNPs@NC and AuNP@NC, respectively) were successfully synthesized by employing DANCs as reducing agent as well as stabilizing template (Fig. 1). The catalytic activity of obtained PdNPs@NCFs nanohybrid for Suzuki coupling reaction was subsequently investigated. To our best knowledge, this paper is the first demonstration for the reduction of Pd (II) and Au (III) ions by DANCs. The present strategy provides a new way to synthesize Pd and Au NPs nanoparticles by cellulose based materials.

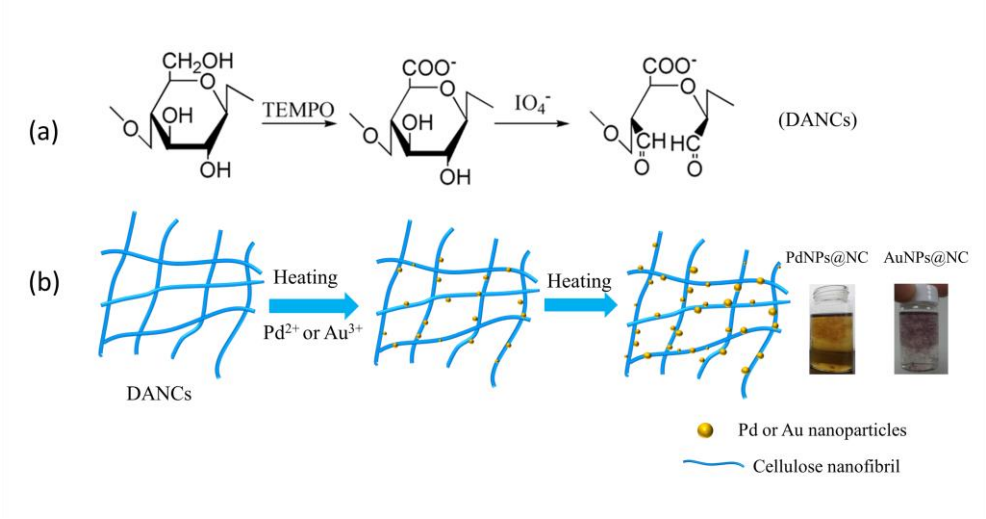

Fig. 1. Schematic illustration of preparation of (a) dialdehyde nanocellulose (DANCs) and (b) PdNPs@NC or AuNPs@NC

2. Materials and methods

2.1. Materials

Bleached sugarcane bagasse sulphite pulp was obtained from Jiangmen sugarcane chemical factory (group) Co.,Ltd. The cellulose content was 94% and the rest was mostly hemicelluloses. 2,2,6,6-tetramethylpiperidinyl-1-oxy radical (TEMPO), 4-nitrophenols (4-NP), odium bromide (NaBr), sodium hypochlorite solution (NaClO, 15%), sodium periodate ($NaIO_4$), potassium carbonate (K_2CO_3), palladium chloride ($PdCl_2$), gold chloride tetrahydrate ($HAuCl_4 \cdot 4H_2O$), HCl, and NaOH were supplied by Sigma–Aldrich and used without further purification. Bromobenzene, bromoanisole, bromobenzonitrile p-bromonitrobenzene and phenylboronic acid were all purchased from Aladdin reagent Co., Ltd. (Shanghai, China).

2.2 Methods

2.2.1 Isolation of cellulose nanofibrils (CNFs) by TEMPO-mediated oxidation

Bleached sugarcane bagasse sulphite pulp was used as a cellulose raw material and cut into small pieces by a crusher. TEMPO-mediated oxidation employing 7 mmol NaClO per gram of cellulose and ultrasonic treatment (sonicating for 30 min with an output power of 450 W and 6 mm probe tip diameter) were subsequently performed as reported before to obtain CNFs (Zhang et al., 2016). The carboxyl content of CNFs obtained was determined to be 1.38 mmol/g cellulose by conductometric titration.

2.2.2. Preparation of 2, 3-dialdehyde nanocelluloses (DANCs) by periodate oxidation

0.4 g $NaIO_4$ was dissolving in 20 mL of aq. 0.6 wt.% CNFs suspension in a brown bottle. The mixture was stirred and reacted under 25°C for 72 h in the dark. The suspension of DANCs was finally obtained after dialyzing against distilled water for 5–7 days to remove excess unreacted sodium periodate (Lu, Li, Chen, & Yu, 2014). The aldehyde content of DANCs was evaluated via the titrimetric method based on Schiff base reactions with hydroxylamine. 0.12 g freeze-dried DANCs was added in a hydroxylamine hydrochloride solution (1 g in 50 mL methanol) with thymol blue as indicator. The mixture was stirred at 40°C for 4 h and then immediately titrated using 0.03 mol/L NaOH methanol solution until a faint pink color was obtained. The aldehyde group content of the synthesized DANCs was 3.8 mmol/g cellulose.

2.2.3. Synthesis of Pd and Au NPs supported on nanocelluloses (PdNPs@NCFs and AuNPs@NCFs)

DANCs suspension was simply diluted with water to 0.1, 0.2 and 0.4 wt.% in three bottles. 10 mL 2 mmol/L Pd (II) complexes in liquid-ammonia $[Pd(NH_3)_4]^{2+}$ (0.035 g of $PdCl_2$ was dissolved in 1 ml of 20% liquid ammonia solution and then diluted into

100 ml with water) was mixed with 10 mL three suspensions (0.1, 0.2 and 0.4 wt.%) of DANCs, respectively. The mixtures were heated to 90°C and reacted for 10 h. For synthesis of AuNPs@NC, 10mL 2 mmol/L $HAuCl_4$ was added into 10 mL of DANCs suspension (0.2 wt.%) under magnetic stirring for 10 h at 90°C. After the reactions, the resulting precipitate PdNPs@NC or AuNPs@NC hybrids were washed and separated from the suspensions by centrifugation at 10 000 g using ethanol. This process was repeated three times to remove the unbound metal nanoparticles.

2.2.4. Catalytic performance of PdNPs@NCFs for Suzuki cross-couplings reaction

Phenylboronic acid (1.5 mmol), aryl bromide (1 mmol), K_2CO_3 (3 mmol), deionized water (9 mL), and 6 mL PdNPs@NCFs hybrid in ethanol (containing 0.0025 mmol palladium), were added to a 25 mL round-bottom flask equipped with a magnetic stirrer. The reaction was refluxed under stirring at 80°C for 2 h. After the reaction was complete, the mixture was cooled down in a water bath under stirring and then dissolved in ethyl acetate. Raw biphenyl compounds were obtained after filtering, leach and concentration of ethyl acetate solution. Finally, the raw biphenyl compounds were purified by passing through column of silica gel.

3. Characterization

Fourier transform infrared (FTIR) spectra of nanocellulosic samples were recorded by a Nicolet iS10 in the range of 400 cm^{-1} to 4000 cm^{-1} with a resolution of 4 cm^{-1}. The UV–vis spectra of PdNPs@NC and AuNPs@NC suspensions were taken at room temperature from 200 to 350 nm using a Shimadzu UV-vis spectrometer (UV-2450). The morphology of DANCs, PdNPs@NC or AuNPs@NC was viewed by JET-1400

transmission electron microscopy (TEM, Hitachi, Japan) at an acceleration voltage of 100 kV. A dilute sample dispersion was deposited on a carbon coated copper grid and left for 3 min after which excess liquid was removed. X-ray diffraction (XRD) patterns of the freeze-dried PdNPs@NC and AuNPs@NC were done on a Siemens D5000 rotating anode wide angle X-ray diffract meter (1 to 120 degrees 2θ). X-ray photoelectron spectroscopy (XPS) experiments were performed by ESCALABMK spectrometer (VG, England) using Mg Kα (1486.6 eV) radiation at 12 kV × 15 mA. The binding energies of the photoelectrons were calibrated by the aliphatic adventitious hydrocarbon C (1s) peak at 284.6 eV. The structures of biphenyl compounds were confirmed by ^{1}H NMR and comparison with authentic samples available commercially or prepared according to literature methods.

4. Result and discussion

4.1 Characterization of cellulose nanofibrils (CNFs), PdNPs@NC and AuNP@NC

The morphologies of CNFs and DANCs were characterized by TEM. Fig. 2a shows the TEM images of CNFs prepared by TEMPO mediated oxidation, where typical CNFs with a diameter in range of 5-20 nm were observed. After periodate oxidation, the morphology of DANCs obtained was basically unchanged compared to original CNFs (Fig. 2b), indicating that the periodate oxidation had little effects on the size of nanocelluloses.

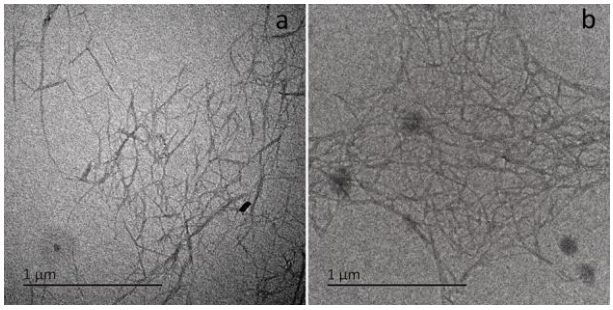

Fig. 2. TEM images of nanocellulosic samples: (a) CNFs prepared by TEMPO-oxidation and (b) DANCs

10 mL 0.1, 0.2 and 0.4 wt.% of DANCs were mixed with 10 mL 2 mmol/L Pd (II) solution, and reacted at 90°C for 10 h to obtain PdNPs@NC. For comparison, 10 mL 0.4 wt.% neat CNFs, which were not treated with sodium periodate, were also reacted with 2 mmol/L Pd (II) at 90°C for 10 h. Photographs of the resulted suspensions are shown in Fig. 3. After 1 h reaction, the appearance of the reaction mixtures in the presence of DANCs (0.1, 0.2 and 0.4 wt.%) changed from colorless to yellowish-brown while the color of suspension of neat CNFs/Pd (II) mixture was unchanged even after 10 h, suggesting that Pd ions could be easily reduced by DANCs but not CNFs (X. D. Wu et al., 2013). Similarly, DANCs/Au (III) reaction mixture changed from colorless to red burgundy indicating the formation of Au NPs. Moreover, visible nanocelluoses aggregates were also observed in all DANCs reacting systems after reacting for 10 h. This phenomenon was probably because of crosslinking of adjacent nanofibrils due to the formation of inter- and intra-molecular hemiacetal linkages of between OH and aldehyde groups, which in turn resulted in the precipitation of cellulose nanofibrils (Sirvio, Liimatainen, Visanko, & Niinimaki, 2014).

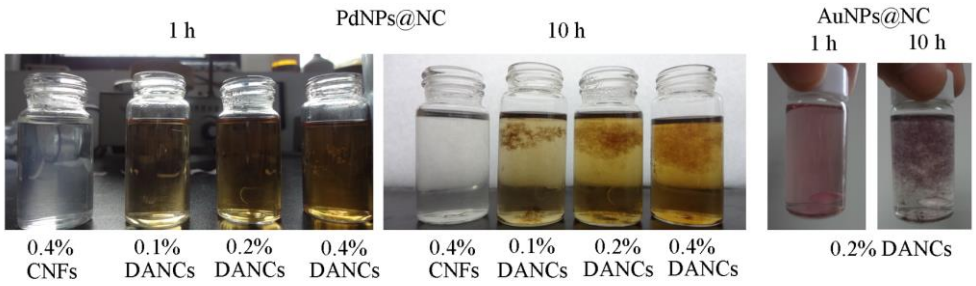

Fig. 3. Photographs of suspensions of palladium or gold nanoparticles coated on nanocellulose (PdNPs@NC and AuNPs@NC) after reaction for 1 and 10 h

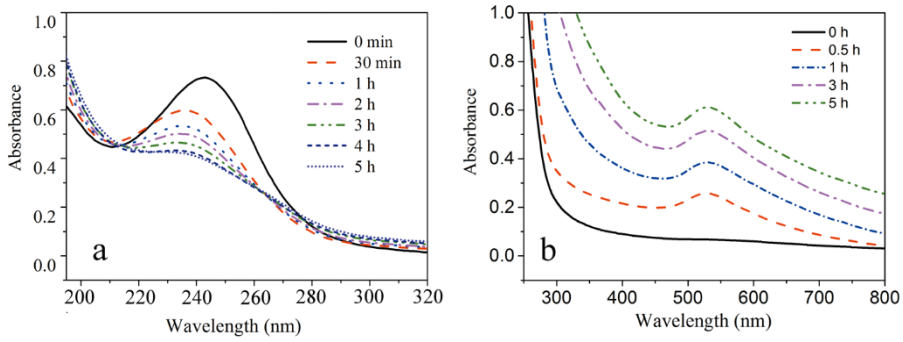

Fig. 4. UV-vis spectra of suspensions of (a) DANCs/Pd (II) and (a) DANCs/Au (III) after different reaction times

In order to monitor the reduction of Pd (II) and Au (III) by DANCs, the ultraviolet-visible absorption spectra of suspensions of (a) DANCs/Pd (II) and (b) DANCs/Au (III) after reacting for different times were recorded, respectively. 10 mL 0.01 mmol/L Pd (II) solution was reacted with 0.05 wt.% DANCs at 40^{o}C, the UV-Vis spectra of these reaction mixtures are shown in Fig. 4. Before the reaction, an absorption peak at around 243 nm, characteristic of Pd (II) ion, was observed in Pd (II)/DANCs solution. With increasing reaction time, the peak gradually disappeared and shifted from 243 to 234 nm after 5 h, which was attributed to the reduction of Pd (II) to Pd (0) (X. D. Wu et al., 2013). For DANCs/Au (III) suspension, an absorption band at 536 nm, which corresponds to the surface plasmon resonance (SPR) band of

the Au NPs (Chen et al., 2017), appeared and increased with the reaction time (from 0 to 5 h). Both the UV-vis spectra of the two suspensions suggested that Pd (II) and Au (III) ions were successfully reduced by DANCs.

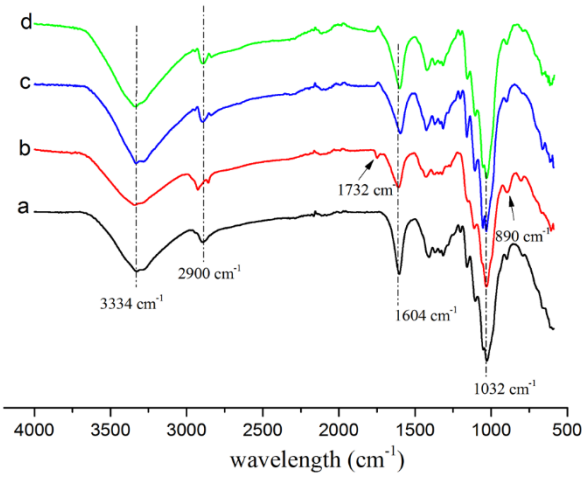

Fig. 5. FT-IR spectra of (a) CNFs, (b) DANCs, (c) PdNPs@NC and (d) AuNPs@NC

FTIR spectra of CNFs, DANCs, PdNPs@NC and AuNPs@NC are presented in Fig. 5. All four samples displayed the typical characteristic of cellulose. The broad bands near to 3326 cm^{-1} are O–H stretching vibrations while the peaks at 2902 cm^{-1} are due to C–H stretching vibrations. The sharp peaks at around 1032 cm^{-1} are related to C–O stretching vibrations. The absorbance band at 1603 cm^{-1} that is characteristic of the sodium carboxylate group, originating from the TEMPO-mediated oxidation (Zhang et al., 2016). The peak of DANCs at 1732 cm^{-1} corresponds to the C=O stretching frequency of free aldehyde (J. Wu et al., 2014). Furthermore, the peak at 889 cm^{-1} is stronger for DANCs than that of original nanocellulose because of the hemiacetal and hydrated form of the DANCs (Liimatainen, Visanko, Sirviö, Hormi, & Niinimaki, 2012). These alterations confirms the success of the surface modification of nanocellulose with aldehyde groups via periodate oxidation. For PdNPs@NC and

AuNPs@NC samples, the absorbance at 1740 cm^{-1} related to aldehyde group disappears. This is attributed to the redox reaction between aldehyde groups and metal ions, in which the aldehyde groups were oxidized to carboxylate groups and the metals ions (Pd^{2+} and Au^{3+}) were reduced to metallic forms (Visanko et al., 2014).

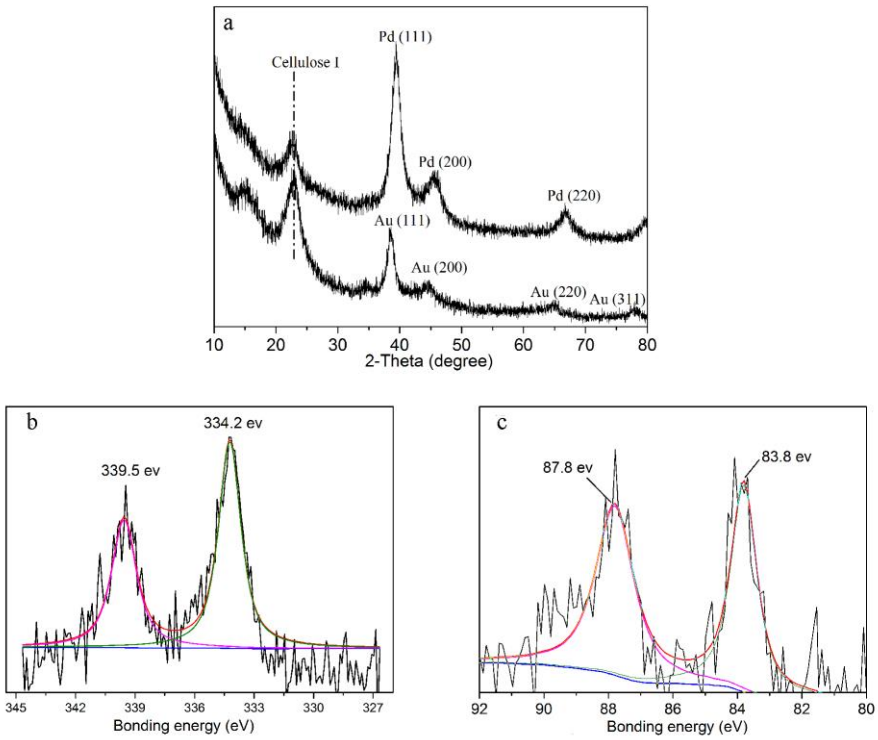

Fig. 6. a) XRD patterns of PdNPs@NC and AuNPs@NC; b) XPS spectrum of PdNPs@NC; c) XPS spectrum of AuNPs@NC nanohybrids

To confirm the formation of Pd or Au NPs on the surface of nanocellulose, the XRD and XPS measurements of freeze-dried PdNPs@NC and AuNPs@NC nanohybrids were performed and the results are shown in Fig. 6. Both the PdNPs@NC and AuNPs@NC nanohybrids show a peak at 22.7º corresponding to the (200) diffraction plane of cellulose I (Wu et al., 2016). Three additional reflections at 40.5, 46.9, and 68.2º were observed in PdNPs@NC sample, which are assigned to diffractions from the (111), (200), and (220) lattice planes of the Pd (0) (Li et al.,

2017). Meanwhile, the pattern for AuNPs@NC displayed a series of peaks at 38.2°, 44.4°, 64.6°, and 77.6°, which are associated with the characteristic (111), (200), (220), and (311) lattice plane for Au (0) crystals (Hu et al., 2017). The reduction of Pd and Au ions were further validated by X-ray photo-electron spectroscopy, which was employed to define the oxidation state of the adsorbed Pd and Au. As shown in Fig. 6b, two peaks located at 339.5 and 334.2 ev, which correspond to the $3d_{5/2}$ and $3d_{7/2}$ of Pd (0) (Zhou et al., 2012), were observed, while no peaks of Pd (II) (near at 337 and 342.1 eV) were found. Similarly, the XPS spectrum of AuNPs@NC presented two high intensity peaks at 83.8 eV and 87.8 eV due to the characteristics signs of Au (0) $4f_{7/2}$ and Au (0) $4f_{5/2}$, and the Au4f peaks of Au (III) at 86.9 eV and 90.6 eV were not observed, neither (Yan et al., 2016). In summary, the results confirmed that the oxidation state of Pd and Au in the freshly prepared nanohybrids were Pd^0 and Au^0, respectively. In other words, the Pd (II) and Au (III) ions were successfully reduced to metallic forms by DANCs as demonstrated above.

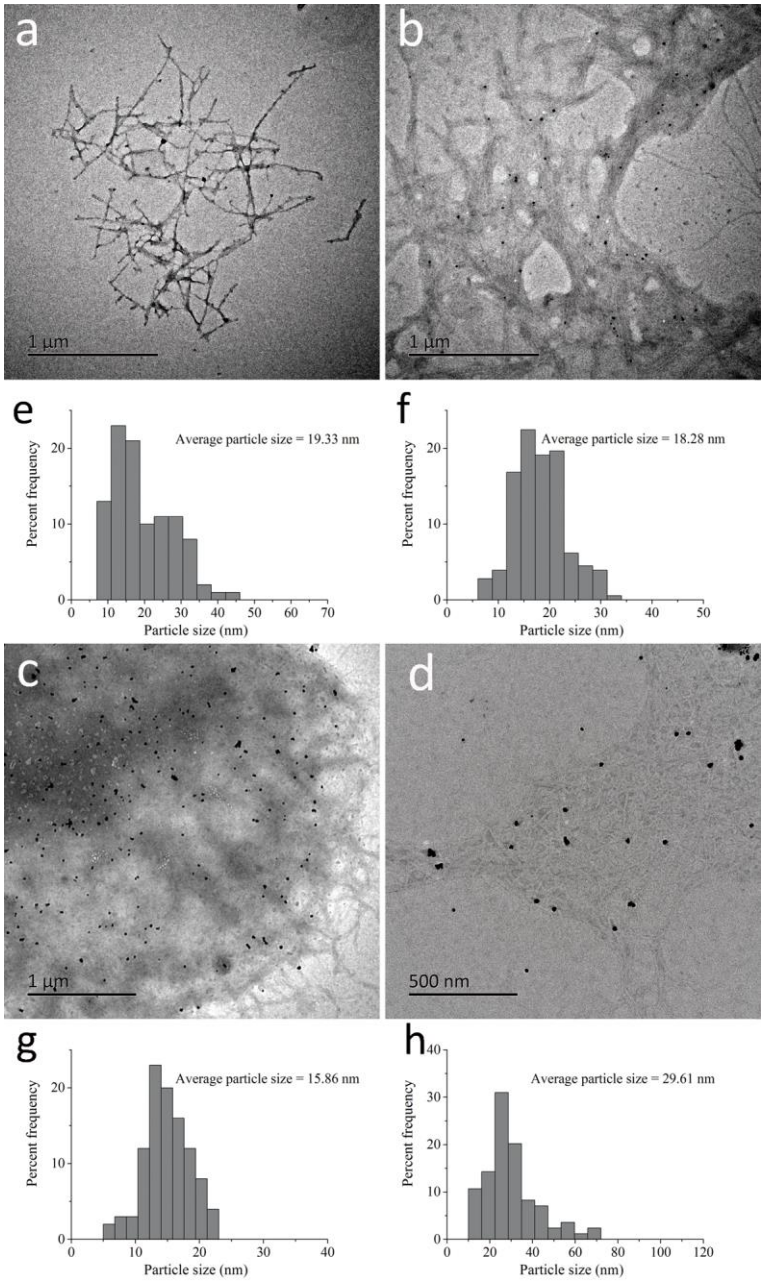

Fig. 7. TEM images and size histograms of PdNPs synthesized by using different DANCs concentrations: (a, e) 0.1 wt.%, (b, f) 0.2 wt.%, and (c, g) 0.4 wt.%; (d, h) AuNPs@NC at DANCs concentration of 0.2 wt.%

TEM images of PdNPs@NC and AuNPs@NC synthesized by DANCs are shown in Fig. 7. Among all PdNPs@NC samples, although the image shows some aggregration of nanocellulose fibers, the obtained Pd NPs were homogeneously

distributed on the surface of nanocelluloses without significant amount of NPs aggregates (Fig. 7a-c). With the increase of the DANCs concentration, more Pd nanoparticles were formed and the average particle size of Pd NPs was slightly decreased. The average particle size of Pd NPs in 0.1, 0.2 and 0.4 wt.% DANCs was 19.33, 18.28 and 15.86 nm, respectively (Fig. 7e-g). Likewise, spherical Au NPs (29.61 nm in average diameter) were also obtained and well deposited onto the surface of nanocellulose (Fig.7d). These results demonstrated that not only DANCs can serve as reducing agent for Pd and Au ions but also stabilizing substrate for formed nanoparticles. On the one hand, the aldehyde groups on the surface of DANCs serve as reducing agent for Pd or Au ions. On the other hand, the carboxylate functionalities derived from TEMPO oxidation can act as anchor sites for Pd or Au NPs (Koga et al., 2010).

4.2 Catalytic activity of PdNPs@NC in Suzuki reaction

Suzuki reactions between phenylboronic acid and different aryl bromides were carried out to address the catalytic performance of resultant PdNPs@NC nanohybrid. The PdNPs@NC used here was prepared by 0.2 wt.% DANCs described above (average particle size is 18.28 nm and Pd content in the hybrid is 1.7 wt.% measured by ICP-AES). Five different aryl bromides (bromobenzene, bromobenzoic acid nitrile, p-bromophenyl methyl ether, bromo-4-nitrobenzene and p-bromo benzaldehyde) were selected the test substrates. Reactions were conducted at 80^{o}C for a total of 2 hours in the presence of 0.1 mol% newly synthesized PdNPs@NC (Table 1). As seen in Table 1, the aryl bromides were all converted to the corresponding biaryls with excellent

yields (more than 90%) after 1 h. Further, product yields in all cases were higher than 95% after 2 h reaction. The comparison of synthesized Pd NP@NC to other Pd−Cellulose catalysts for the Suzuki reaction is also shown in Table 2. Direct comparison of this catalyst to other palladium nanoparticle/cellulose catalysts developed by other reseachers is difficult due to the different preparation conditions of the catalysts and coupling reaction conditions. However, even with a larger particle size, the synthesized PdNPs@NC produced a relatively high reaction yield with lower reaction time or smaller amount of catalyst in comparison to previously reported results (Table 2).

Table 1. Suzuki Coupling of aryl bromides and phenylboronic acid using PdNPs@NC[a]

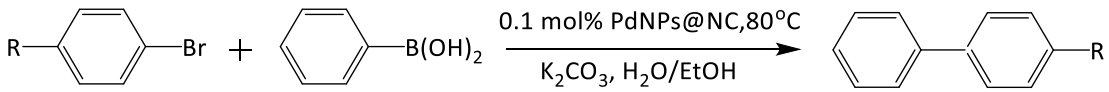

Sample	R	Time (h)	Yield (%)
1	H	1	96
2	H	2	100
3	NO_2	1	97
4	NO_2	2	99
5	CHO	1	95
6	CHO	2	99
7	OCH_3	1	94
8	OCH_3	2	98
9	CN	1	96
10	CN	2	99

[a]Reaction condition: aryl halides (1 mmol), phenylboronic acid (1.5 mmol), H_2O/EtOH (3:2), K_2CO_3 (3 mmol) and aerobic conditions.

Table 2. Comparison of Pd−Cellulose catalysts for the Suzuki reaction

Catalyst	Pd NPs Size (nm)	Reaction conditions	Amount of catalyst	Yield	Reference
Cellulose-supported nano Pd(0)	5	K_2CO_3, water, 100°C, 12 h	0.3 mol%	90%	Jamwal, Sodhi, Gupta, & Paul (2011)
Palladium incorporated into cellulose–Al2O3	no data	K_2CO_3, H_2O, 80°C, 2 h	1 mol%	96%	Kumbhar et al. （2013）
Cellulose-N-heterocyclic carbenes-palladium catalyst	9	K_2CO_3, EtOH:H_2O (1:1), 80°C, 2 h	0.75 mol%	86%	Wang, Hu, Xue, & Wei, (2014)
Immobilize Pd NPs on cellulose sponge	2.5	K_2CO_3, EtOH:H_2O (1:1), 65°C, 3 h	1 mmol%	99%	Li et al. (2017)
Pd NPs@NC	18.3	K_2CO_3, EtOH:H_2O (2:3), 80°C, 1 h	0.1 mol%	96%	This work

5. Conclusions

In this study, we described a facile synthetic approach that involves the use of dialdehyde nanocelluloses (DANCs) for the synthesis of PdNPs@NC and AuNPs@NC for the first time. Herein, DANCs acted not only as reducing agent but also as template for the reduction and deposition of Pd and Au NPs. XRD and XPS confirmed that Pd (II) and Au (III) ions were successfully reduced to metallic Pd^0 and

Au^0. TEM images revealed that synthesized Pd and Au NPs were well dispersed on the surface of cellulose nanofibrils. Additionally, for PdNPs@NC cases, with the increase of the DANCs concentration, more Pd nanoparticles were formed and the average particle size of Pd NPs was slightly decreased. Moreover, the synthesized PdNPs@NC nanohybrid showed an excellent catalytic activity in Suzuki coupling reaction.

Notes

The authors declare no competing financial interest.

Acknowledgements

The authors would like to thank the National "Twelfth Five-Year" Plan for Science & Technology Support of China (2015BAD14B06) and Academy of Finland for funding (Project No. 307086).

References

Benaissi, K., Johnson, L., Walsh, D. A., & Thielemans, W. (2010). Synthesis of platinum nanoparticles using cellulosic reducing agents. *Green Chemistry*, 12(2), 220-222.

Chen, L., Cao, W. J., Quinlan, P. J., Berry, R. M., & Tam, K. C. (2015). Sustainable catalysts from gold-loaded polyamidoamine dendrimer-cellulose nanocrystals. *Acs Sustainable Chemistry & Engineering*, 3(5), 978-985.

Chen, M. Y., Kang, H. L., Gong, Y. M., Guo, J., Zhang, H., & Liu, R. G. (2015). Bacterial cellulose supported gold nanoparticles with excellent catalytic properties. *Acs Applied Materials & Interfaces*, 7(39), 21717-21726.

Chen, Y.; Chen, S. Y.; Wang, B. X.; Yao, J. J.; Wang, H. P. (2017). TEMPO-oxidized bacterial cellulose nanofibers-supported gold nanoparticles with superior catalytic properties. *Carbohydrate Polymers*, 160, 34-42.

Cirtiu, C. M., Dunlop-Briere, A. F., & Moores, A. (2011). Cellulose nanocrystallites as an efficient support for nanoparticles of palladium: application for catalytic hydrogenation and Heck coupling under mild conditions. *Green Chemistry*, 13(2), 288-291.

Del Zotto, A., & Zuccaccia, D. (2017). Metallic palladium, PdO, and palladium supported on metal oxides for the Suzuki-Miyaura cross-coupling reaction: a

346 unified view of the process of formation of the catalytically active species in
347 solution. *Catalysis Science & Technology*, 7(18), 3934-3951.
348 Dong, Y. Y., Liu, S., Liu, Y. J., Meng, L. Y., & Ma, M. G. (2017).
349 Ag@Fe_3O_4@cellulose nanocrystals nanocomposites: microwave-assisted
350 hydrothermal synthesis, antimicrobial properties, and good adsorption of dye
351 solution. *Journal of Materials Science*, 52(13), 8219-8230.
352 Dong, Z. P., Le, X. D., Dong, C. X., Zhang, W., Li, X. L., & Ma, J. T. (2015). Ni@Pd
353 core-shell nanoparticles modified fibrous silica nanospheres as highly efficient and
354 recoverable catalyst for reduction of 4-nitrophenol and hydrodechlorination of
355 4-chlorophenol. *Applied Catalysis B-Environmental*, 162, 372-380.
356 Drogat, N., Granet, R., Sol, V., Memmi, A., Saad, N., Koerkamp, C. K., Krausz, P.
357 (2011). Antimicrobial silver nanoparticles generated on cellulose nanocrystals.
358 *Journal of Nanoparticle Research*, 13(4), 1557-1562.
359 Fu, L. H., Deng, F., Ma, M. G., & Yang, J. (2016). Green synthesis of silver
360 nanoparticles with enhanced antibacterial activity using holocellulose as a substrate
361 and reducing agent. *Rsc Advances*, 6(34), 28140-28148.
362 Ghaderi, A., Gholinejad, M., & Firouzabadi, H. (2016). Palladium deposited on
363 naturally occurring supports as a powerful catalyst for carbon-carbon bond
364 formation reactions. *Current Organic Chemistry*, 20(4), 327-348.
365 Hassan, J., Sévignon, M., Gozzi, C., Schulz, E., & Lemaire, M. (2002). Aryl−Aryl
366 bond formation one century after the discovery of the ullmann reaction. *Chemical*
367 *Reviews*, 102(5), 1359-1470.
368 He, J., Kunitake, T., & Nakao, A. (2003). Facile in situ synthesis of noble metal
369 nanoparticles in porous cellulose fibers. *Chemistry of Materials*, 15(23),
370 4401-4406.
371 Hu, Z., Meng, Q., Liu, R., Fu, S., & Lucia, L. A. (2017). Physical study of the
372 primary and secondary photothermal events in gold/cellulose nanocrystals
373 (AuNP/CNC) nanocomposites embedded in PVA matrices. *Acs Sustainable*
374 *Chemistry & Engineering*, 5(2), 1601-1609.
375 Jamwal, N., Sodhi, R. K., Gupta, P., & Paul, S. (2011). Nano Pd(0) supported on
376 cellulose: A highly efficient and recyclable heterogeneous catalyst for the Suzuki
377 coupling and aerobic oxidation of benzyl alcohols under liquid phase catalysis.
378 *International Journal of Biological Macromolecules*, 49 (5), 930-935.
379 Kaushik, M., & Moores, A. (2016). Review: nanocelluloses as versatile supports for
380 metal nanoparticles and their applications in catalysis. *Green Chemistry*, 18(3),
381 622-637. R.Salunkhe.
382 Kumbhar, S., Jadhav, S., Kamble, G., & Rashinkar, R.Salunkhe. (2013). Palladium
383 supported hybrid cellulose-aluminum oxide composite for Suzuki-Miyaura cross
384 coupling reaction. *Tetrahedron Letters*, 54 (11), 1331-1337.
385 Koga, H., Tokunaga, E., Hidaka, M., Umemura, Y., Saito, T., Isogai, A., & Kitaoka,
386 T. (2010). Topochemical synthesis and catalysis of metal nanoparticles exposed on
387 crystalline cellulose nanofibers. *Chemical Communications*, 46(45), 8567-8569.

Li, M.-C., Wu, Q., Song, K., Lee, S., Qing, Y., & Wu, Y. (2015). Cellulose nanoparticles: structure–morphology–rheology relationships. *Acs Sustainable Chemistry & Engineering*, 3(5), 821-832.

Li, P., Sirviö, J. A., Haapala, A., & Liimatainen, H. (2017). Cellulose nanofibrils from nonderivatizing urea-based deep eutectic solvent pretreatments. *ACS Applied Materials and Interfaces*, 9(3), 2846-2855.

Li, Y., Xu, L., Xu, B., Mao, Z., Xu, H., Zhong, Y., Sui, X. (2017). Cellulose sponge supported palladium nanoparticles as recyclable cross-coupling catalysts. *Acs Applied Materials & Interfaces*, 9(20), 17155-17162.

Liimatainen, H., Sirvio, J., Pajari, H., Hormi, O., & Niinimaki, J. (2013). Regeneration and recycling of aqueous periodate solution in dialdehyde cellulose production. *Journal of Wood Chemistry and Technology*, 33(4), 258-266.

Liimatainen, H., Visanko, M., Sirviö, J. A., Hormi, O. E. O., & Niinimaki, J. (2012). Enhancement of the nanofibrillation of wood cellulose through sequential periodate-chlorite oxidation. *Biomacromolecules*, 13(5), 1592-1597.

Liu, H., Song, J., Shang, S. B., Song, Z. Q., & Wang, D. (2012). Cellulose nanocrystal/silver nanoparticle composites as bifunctional nanofillers within waterborne polyurethane. *Acs Applied Materials & Interfaces*, 4(5), 2413-2419.

Liu, Y. X., Yang, X. J., Liu, H. Y., Ye, Y. H., & Wei, Z. J. (2017). Nitrogen-doped mesoporous carbon supported Pt nanoparticles as a highly efficient catalyst for decarboxylation of saturated and unsaturated fatty acids to alkanes. *Applied Catalysis B-Environmental*, 218, 679-689.

Loh, G. C. (2016). Electronic and magnetic properties of encapsulated MoS_2 quantum dots: The case of noble metal nanoparticle dopants. *Chemphyschem*, 17(8), 1180-1194.

Long, N. V., Thi, C. M., Yong, Y., Nogami, M., & Ohtaki, M. (2013). Platinum and palladium nano-structured catalysts for polymer electrolyte fuel cells and direct methanol Fuel Cells. *Journal of Nanoscience and Nanotechnology*, 13(7), 4799-4824.

Lu, T. H., Li, Q., Chen, W. S., & Yu, H. P. (2014). Composite aerogels based on dialdehyde nanocellulose and collagen for potential applications as wound dressing and tissue engineering scaffold. *Composites Science and Technology*, 94, 132-138.

Mou, K., Li, J., Wang, Y., Cha, R., & Jiang, X. (2017). 2,3-Dialdehyde nanofibrillated cellulose as a potential material for the treatment of MRSA infection. *Journal of Materials Chemistry B*, 5(38), 7876-7884.

Nadagouda, M. N., & Varma, R. S. (2008). Green synthesis of silver and palladium nanoparticles at room temperature using coffee and tea extract. *Green Chemistry*, 10(8), 859-862.

Phan, N. T. S., Van Der Sluys, M., & Jones, C. W. (2006). On the nature of the active species in palladium catalyzed mizoroki–heck and suzuki–miyaura couplings – homogeneous or heterogeneous catalysis, a critical review. *Advanced Synthesis & Catalysis*, 348(6), 609-679.

Rezayat, M., Blundell, R. K., Camp, J. E., Walsh, D. A., & Thielemans, W. (2014). Green one-step synthesis of catalytically active palladium nanoparticles supported

on cellulose nanocrystals. *Acs Sustainable Chemistry & Engineering*, 2(5), 1241-1250.

Sarina, S., Waclawik, E. R., & Zhu, H. Y. (2013). Photocatalysis on supported gold and silver nanoparticles under ultraviolet and visible light irradiation. *Green Chemistry*, 15(7), 1814-1833.

Shi, Z. Q., Tang, J. T., Chen, L., Yan, C. R., Tanvir, S., Anderson, W. A., Tam, K. C. (2015). Enhanced colloidal stability and antibacterial performance of silver nanoparticles/cellulose nanocrystal hybrids. *Journal of Materials Chemistry B*, 3(4), 603-611.

Shimizu, K., Koizumi, S., Hatamachi, T., Yoshida, H., Komai, S., Kodama, T., & Kitayama, Y. (2004). Structural investigations of functionalized mesoporous silica-supported palladium catalyst for Heck and Suzuki coupling reactions. *Journal of Catalysis*, 228(1), 141-151.

Sirviö, J. A., Visanko, M., & Liimatainen, H. (2015). Deep eutectic solvent system based on choline chloride-urea as a pre-treatment for nanofibrillation of wood cellulose. *Green Chemistry*, 17(6), 3401-3406.

Sirvio, J., Liimatainen, H., Niinimaki, J., & Hormi, O. (2011). Dialdehyde cellulose microfibers generated from wood pulp by milling-induced periodate oxidation. *Carbohydrate Polymers*, 86(1), 260-265.

Sirvio, J. A., Liimatainen, H., Visanko, M., & Niinimaki, J. (2014). Optimization of dicarboxylic acid cellulose synthesis: Reaction stoichiometry and role of hypochlorite scavengers. *Carbohydrate Polymers*, 114, 73-77.

Sirvio, J. A., & Visanko, M. (2017). Anionic wood nanofibers produced from unbleached mechanical pulp by highly efficient chemical modification. *Journal of Materials Chemistry A*, 5(41), 21828-21835.

Suopajärvi, T., Sirviö, J. A., & Liimatainen, H. (2017). Cationic nanocelluloses in dewatering of municipal activated sludge. *Journal of Environmental Chemical Engineering*, 5(1), 86-92.

Van Rie, J., & Thielemans, W. (2017). Cellulose-gold nanoparticle hybrid materials. *Nanoscale*, 9(25), 8525-8554.

Visanko, M., Liimatainen, H., Sirvio, J. A., Haapala, A., Sliz, R., Niinimaki, J., & Hormi, O. (2014). Porous thin film barrier layers from 2,3-dicarboxylic acid cellulose nanofibrils for membrane structures. *Carbohydrate Polymers*, 102, 584-589.

Visanko, M., Sirviö, J. A., Piltonen, P., Sliz, R., Liimatainen, H., & Illikainen, M. (2017). Mechanical fabrication of high-strength and redispersible wood nanofibers from unbleached groundwood pulp. *Cellulose*, 24(10), 4173-4187.

Wang, X., Hu,P., Xue,F., & Wei,F. (2014), Cellulose-supported N-heterocyclic carbene-palladium catalyst: Synthesis and its applications in the Suzuki cross-coupling reaction. *Carbohydrate Polymers*, 114, 476-483.

Wang, M. Y., Ye, M. D., Iocozzia, J., Lin, C. J., & Lin, Z. Q. (2016). Plasmon-mediated solar energy conversion via photocatalysis in noble metal/semiconductor composites. *Advanced Science*, 3(6), 14.

Wu, B., Kuang, Y., Zhang, X., & Chen, J. (2011). Noble metal nanoparticles/carbon nanotubes nanohybrids: Synthesis and applications. *Nano Today*, 6(1), 75-90.

Wu, M., Kuga, S., & Huang, Y. (2008). Quasi-one-dimensional arrangement of silver nanoparticles templated by cellulose microfibrils. *Langmuir*, 24(18), 10494-10497.

Wu, X., Shi, Z., Fu, S., Chen, J., Berry, R. M., & Tam, K. C. (2016). Strategy for synthesizing porous cellulose nanocrystal supported metal nanocatalysts. *Acs Sustainable Chemistry & Engineering*, 4(11), 5929-5935.

Wu, X. D., Lu, C. H., Zhang, W., Yuan, G. P., Xiong, R., & Zhang, X. X. (2013). A novel reagentless approach for synthesizing cellulose nanocrystal-supported palladium nanoparticles with enhanced catalytic performance. *Journal of Materials Chemistry A*, 1(30), 8645-8652.

Wu, X. D., Lu, C. H., Zhou, Z. H., Yuan, G. P., Xiong, R., & Zhang, X. X. (2014). Green synthesis and formation mechanism of cellulose nanocrystal-supported gold nanoparticles with enhanced catalytic performance. *Environmental Science-Nano*, 1(1), 71-79.

Xiong, R., Lu, C. H., Zhang, W., Zhou, Z. H., & Zhang, X. X. (2013). Facile synthesis of tunable silver nanostructures for antibacterial application using cellulose nanocrystals. *Carbohydrate Polymers*, 95(1), 214-219.

Xu, L., Wu, X. C., & Zhu, J. J. (2008). Green preparation and catalytic application of Pd nanoparticles. *Nanotechnology*, 19(30), 305603.

Yan, W., Chen, C., Wang, L., Zhang, D., Li, A.-J., Yao, Z., & Shi, L.-Y. (2016b). Facile and green synthesis of cellulose nanocrystal-supported gold nanoparticles with superior catalytic activity. *Carbohydrate Polymers*, 140, 66-73.

Yu, K. K., Sun, X. N., Pan, L., Liu, T., Liu, A. P., Chen, G., & Huang, Y. Z. (2017). Hollow Au-Ag Alloy Nanorices and Their Optical Properties. *Nanomaterials*, 7(9), 8.

Zhang, K., Sun, P., Liu, H., Shang, S., Song, J., & Wang, D. (2016). Extraction and comparison of carboxylated cellulose nanocrystals from bleached sugarcane bagasse pulp using two different oxidation methods. *Carbohydrate Polymers*, 138, 237-243.

Zhou, P., Wang, H., Yang, J., Tang, J., Sun, D., & Tang, W. (2012). Bacteria Cellulose Nanofibers Supported Palladium(0) Nanocomposite and Its Catalysis Evaluation in Heck Reaction. *Industrial & Engineering Chemistry Research*, 51(16), 5743-5748.